machines

Article

Analysis of Stainless-Steel Tape Dynamic Behavior and Its Impact on Raster Scale Formation Accuracy

Donatas Gurauskis [1], Albinas Kasparaitis [2], Edgar Sokolovskij [3,*], Jonas Matijošius [1] and Artūras Kilikevičius [1]

[1] Institute of Mechanical Science, Vilnius Gediminas Technical University, LT-10105 Vilnius, Lithuania; donatas.gurauskis@vilniustech.lt (D.G.); jonas.matijosius@vilniustech.lt (J.M.); arturas.kilikevicius@vilniustech.lt (A.K.)
[2] Department of Mechanical and Material Engineering, Vilnius Gediminas Technical University, LT-10105 Vilnius, Lithuania; albinas.kasparaitis@vilniustech.lt
[3] Department of Automobile Engineering, Vilnius Gediminas Technical University, LT-10105 Vilnius, Lithuania
* Correspondence: edgar.sokolovskij@vilniustech.lt

Abstract: The formation of raster structures on stainless-steel tapes requires high-precision mechatronic systems to ensure accuracy and stability during the process. This article gives a thorough look at a redesigned precise mechatronic system that can make coded or raster linear scales using a dynamic laser process. These scales are critical components in linear measuring systems, such as optical encoders, where accuracy and reliability are paramount. One critical challenge is maintaining precise tape dynamics to mitigate errors caused by slippage at the tape-roller interface and mechanical vibrations. The main goal of this study is to look at these changing behaviors in a redesigned tape displacement measurement unit. Unlike older models, this one does not use a pneumatic roller system; instead, the tape drives the measuring roller directly. Experiments show that the new design greatly lowers errors caused by slippage and vibration, which makes it easier for the tape to move in sync with the laser activation. Additionally, the updated system exhibits enhanced performance in terms of stability, achieving higher accuracy of the raster structure compared to the previous design. These findings underscore the importance of dynamic analysis in optimizing tape displacement measurement units for high-precision raster formation processes.

Keywords: raster scale formation; stainless-steel tape dynamics; tape slippage; vibration analysis

Academic Editor: Kai Cheng

Received: 18 December 2024
Revised: 22 January 2025
Accepted: 4 February 2025
Published: 7 February 2025

Citation: Gurauskis, D.; Kasparaitis, A.; Sokolovskij, E.; Matijošius, J.; Kilikevičius, A. Analysis of Stainless-Steel Tape Dynamic Behavior and Its Impact on Raster Scale Formation Accuracy. *Machines* **2025**, *13*, 124. https://doi.org/10.3390/machines13020124

1. Introduction

Precision measurement systems, like linear optical encoders, need linear stainless-steel tapes with a raster or code structure in order to work. These tapes provide reference scales that enable highly accurate linear displacement measurements across a variety of industries, including automation, robotics, and precision manufacturing. Their robust design and precisely etched structures ensure durability and reliable performance, even in demanding environments.

Stainless steel is the preferred material for these tapes due to its excellent mechanical properties. It is highly durable, resisting wear and corrosion while maintaining flexibility under tension or bending. Stainless steel also exhibits superior thermal stability, ensuring minimal expansion or contraction under temperature changes, which is critical for consistent measurements. There are two types of formed patterns on these tapes: raster structures, which are made up of evenly spaced lines or tracks for incremental positioning, and coded patterns, which can be binary or gray-coded designs for absolute positioning.

The ability to manufacture metal scales in significantly longer lengths compared to glass scales is one of their key advantages. While glass scales are typically limited to lengths of around 3 m due to their fragility and the challenges of producing defect-free substrates over longer spans, stainless-steel scales can easily exceed a few tens of meters in length. This makes them indispensable for applications requiring extensive measurement ranges. For instance, the aerospace industry uses long metal scales for precise positioning during the assembly of large aircraft components [1]. Similarly, in automated conveyor systems, such scales provide accurate displacement measurements over extended distances [2]. Metal scales can be used on large gantry-style CNC machines and coordinate measuring machines (CMMs), which makes sure that measurements are accurate even when the machines are used in large areas [3].

A further advantage of stainless-steel scales over their glass counterparts is their superior ease of transport, handling, and mounting. Metal scales are highly flexible and resistant to breakage, making them more suitable for on-site handling during installation or maintenance. Unlike glass scales, which are fragile and require careful packaging and transportation to prevent damage, metal scales can be coiled into compact rolls, reducing space requirements and minimizing the risk of breakage during shipping. Additionally, their robustness streamlines mounting, particularly in applications that demand long measurement spans or necessitate on-site alignment adjustments. These characteristics make stainless-steel scales an ideal choice for demanding industrial environments.

There are different ways to make raster structures on linear scales, and the one you choose depends on how accurate you need them to be, how much they cost to make, and what you need them for. Common techniques include laser ablation of coatings, printing, and paint application technologies, mechanical scratching, and embossing.

Printing and paint application technologies, such as screen printing and inkjet printing, are widely used for creating raster structures where moderate accuracy suffices. These methods allow for rapid patterning in large areas at low costs, making them suitable for less critical applications. For example, inkjet printing has been used to make electronic parts and straight lines. Measuring scales are made by carefully depositing conductive or reflective inks [4]. Screen printing is another robust method, ideal for thicker coatings or larger features, although it is less suited for sub-micron patterns.

Mechanical scratching and embossing methods are often employed to create robust, durable patterns on metallic or polymeric substrates. These techniques involve physically displacing material to form raster structures, often using precision tools or dies. Mechanical scratching, while cost-effective, typically lacks the resolution of laser ablation or lithography, but it remains useful for industrial settings where durability and visibility are priorities [5]. Embossing, on the other hand, uses prefabricated molds or dies to imprint patterns onto materials. This process is highly scalable and efficient for repetitive tasks but requires significant upfront investment in tooling [6].

For most precision applications, raster structures have a periodicity ranging from 1 μm to 40 μm, with individual line lengths reaching several millimeters. At such high densities and with small line widths, stringent requirements are imposed on the edge quality of the lines. When scanning these precision scales using photoelectric measuring heads, the sharpness and consistency of the edges directly influence signal quality and overall measurement accuracy. Often, applications demanding such precision utilize static lithographic processes. Usually, these steps are used on chromium-coated glass rulers or gold-coated stainless-steel tapes. Lithographic methods are used to make precise scales with clear line dimensions. Recent advancements in lithographic techniques, including extreme ultraviolet (EUV) lithography, have significantly enhanced resolution, paving the way for the creation of nanostructures with feature sizes as small as 10 nm [7]. However, these methods involve complex setups and are typically reserved for semiconductor manufacturing, where such precision is paramount. Laser ablation is a great alternative for making linear scales, where getting the right balance between accuracy and speed is very important [8].

Laser ablation, especially with femtosecond lasers, can remove material with great accuracy, which lets you make complex patterns with features that are less than a micron in size. Dynamically performed, this method offers flexibility and speed, making it suitable for high-throughput manufacturing processes. Traditional lithography methods, like ultraviolet (UV) lithography, have more steps, such as coating the photoresist, exposing the image under a photomask, and developing the image. Generally conducted in a static manner, these steps require precise alignment and can be time-consuming, making them less adaptable to continuous production workflows [9].

The laser etching process is particularly well suited to stainless-steel tapes, combining flexibility, precision, and scalability. It begins with preparing the tapes by cleaning and pre-treating the surface for optimal results. The laser system dynamically feeds the tape under controlled tension and alignment. The laser beam is precisely modulated to ablate the surface and form high-contrast raster or coded patterns. This dynamic approach eliminates the need for stop-and-start operations, significantly improving production efficiency. After etching, the tape is cooled, cleaned, and rewound into a coil for easy handling and storage. Inspection systems integrated into the process ensure that the etched patterns meet stringent quality standards.

In the development of mechatronic manufacturing systems for stainless-steel tapes, precise control of tape displacement is crucial. The real-time feedback mechanism, essential for synchronizing laser operations with tape motion, traditionally comprises a measurement roller. In this setup, the tape is pressed against the roller with a controllable force exerted by an opposing roller, typically actuated by a pneumatic system. Extensive research has been conducted to optimize this unit, focusing on its dynamic parameters, contact mechanics, and vibrational behavior.

A. Fursenko et al. studied how the tape-feeding mechanism moves and emphasized how important it is to know the system's natural frequencies and damping properties to avoid resonant vibrations that could affect the accuracy of the etching process. According to what they found, improving these dynamic parameters makes the raster formation process more stable and accurate [10].

In a different study, A. Fursenko et al. looked at how the tape and measurement roller interacted with each other by measuring things like contact pressure, friction coefficients, and material deformation. To accurately measure tape displacement, which has a direct impact on the quality of the etched patterns [11], the results show that the contact force needs to be carefully controlled, and a deep understanding of how friction works is needed.

Additionally, we conducted an investigation into how variations in frictional conditions affect the vibrational behavior of steel tapes during processing. This study reveals that changes in friction can induce vibrations, leading to potential defects in the etched patterns. Implementing effective friction management strategies is essential to mitigate these vibrations and ensure the precision of the manufacturing process [12].

Collectively, these studies provide valuable insights into the mechanical interactions within the tape displacement measurement unit. However, the final accuracy of the produced scales using such a configuration was unsatisfactory. As a result, we redesigned the tape displacement measurement unit. The new assembly eliminated the pressing roller, as its deformations in the tape were the primary source of error. Now, the tape passes over a guide roller and wraps around the measuring roller, driving its rotation.

Such linear steel tape systems used in mechatronic applications are highly sensitive to mechanical vibrations and slippage, which can adversely affect their precision and operational reliability. Vibrations can originate from both internal and external sources, including motor imbalances, external environmental disturbances, and inherent system resonances [13,14]. These vibrations cause oscillatory behaviors in the tape, leading to positional inaccuracies, disrupted measurements, and potential damage to system components.

The slippage between the tape and roller mechanisms introduces additional challenges, such as inconsistent displacement measurements. This phenomenon is particularly pronounced in systems where maintaining constant tension and adequate contact pressure is difficult [15]. Slippage often results from poor roller alignment, uneven wear, or variations in tape tension during operation. Research shows that optimizing roller geometry and using advanced tension control systems can effectively reduce slippage and improve measurement accuracy [16].

The dynamics of tape slippage and its interplay with vibrations can exacerbate errors in position sensing. For instance, the design of guiding systems and tensioning mechanisms is closely linked to lateral positioning errors caused by vibrations and slippage. Researchers who looked at how tilted rollers affected the movement of tape found that it is very important to carefully adjust the roller angle and the way the tape contacts the rollers in order to keep the tape stable and in the right place [16]. Moreover, the introduction of advanced vibration-damping techniques, such as isolation mounts and damping layers, has been shown to minimize the transmission of vibratory forces to critical components, thereby preserving the accuracy of linear tape systems [17,18].

High-frequency tape vibrations, which are often caused by the material itself and the speed at which it is used, can change the accuracy of displacement measurements [19]. Real-time feedback systems with high-resolution optical encoders are very important for finding these distortions and fixing them, ensuring that measurements are accurate over long periods of time. Slippage and errors caused by vibration can also be stopped from getting worse by using advanced maintenance methods like checking the alignment and roller conditions on a regular basis [20].

This study investigates a new design tape displacement measurement unit to analyze the dynamic behavior of a steel tape and assess potential slippage on the measuring roller. An analysis of the key parameters that ensure stable operation was carried out, along with dynamic testing of the unit under operational conditions and mechanical vibration excitation from the outside. Using advanced metrological measurement systems, the linear velocity of the tape in the raster formation zone and its correlation with the velocity of the measuring roller were examined. The relative and absolute accuracy of the raster structures made by the system with the redesigned unit was also tested. This showed how the updated configuration improved performance and accuracy.

2. Overview

This section presents a detailed examination of the tape displacement measurement unit, its functional role in the precision formation of raster structures, and the dynamic phenomena influencing its performance. The discussion encompasses the research object, identifies principal error sources (slippage and mechanical vibrations), and provides a theoretical framework for understanding their impact on system accuracy. Furthermore, strategies for mitigating these errors are analyzed, and critical system parameters necessary for achieving optimal operational stability and high-quality raster scale generation are summarized.

2.1. Research Object

The thing being looked into is a high-tech and complicated mechatronic device that was made to precisely create raster patterns on a stainless-steel tape using laser technology. The tape, which serves as the substrate for the raster structures, is unwound from a reel and guided through several system components and redirecting rollers. The tape displacement measurement unit is an important part of the system because it makes sure that everything is in sync and lined up correctly for the raster formation process. Figure 1 presents the model view of this unit.

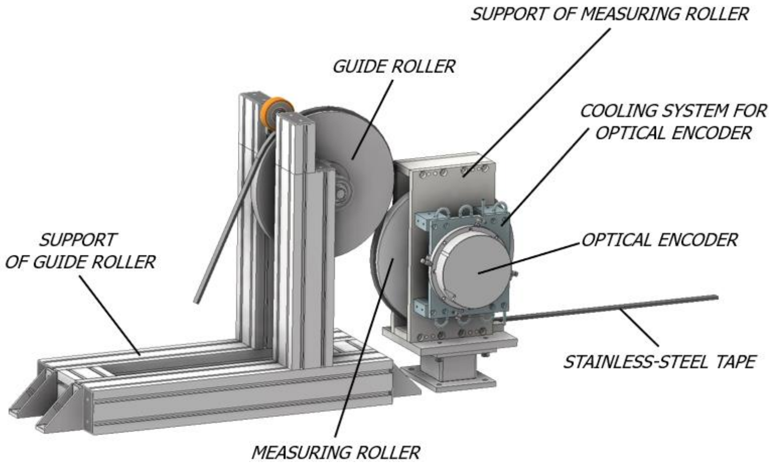

Figure 1. Model view of tape displacement measurement unit.

Within the displacement measurement unit, the tape wraps around a measuring roller, causing it to rotate as the tape moves forward. The measuring roller mounts a precision optical angular encoder, custom-engineered for this device. This encoder converts the roller's rotational motion into precise angular measurements, which are then used to calculate the tape's linear displacement. These calculations are critical for two primary functions: determining the tape's exact position and controlling the activation and modulation of the laser used to form the raster structures.

The dynamic behavior of the tape within this unit is a critical factor in ensuring its proper operation and has been identified as the primary research objective. Investigating the tape's motion stability, including factors such as slippage and vibration effects, is essential to improve the reliability and precision of the tape displacement measurement process. The schematic representation of the tape measurement unit is shown in Figure 2.

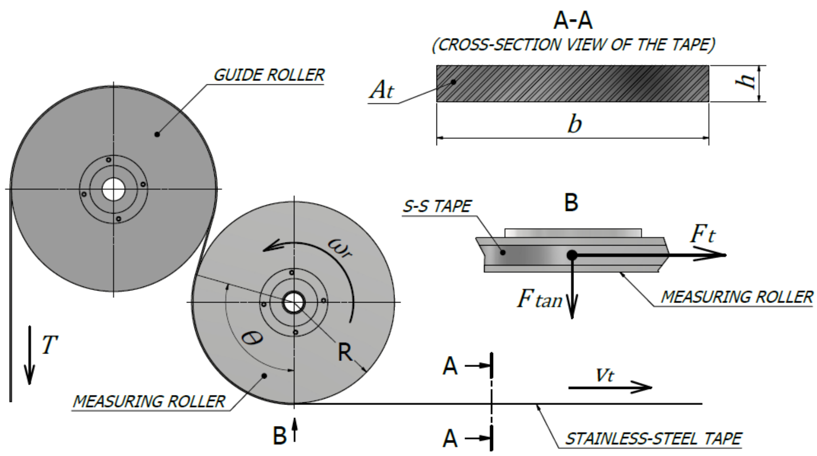

Figure 2. Schematic representation of tape displacement measurement unit.

A metal tape is pulled at one end at a linear operational velocity v_t. At the other end, a precision braking system is installed to maintain a stable tape tension T of the required magnitude. During the process, the tape wraps around the measuring roller (with a radius R) at a specific wrapping angle θ, causing it to rotate at an angular velocity ω_r. This angular velocity of the roller ω_r and the linear velocity of the tape v_t are coupled through:

$$v_t = \mathrm{R}\omega_r, \tag{1}$$

In the contact zone between the measuring roller and the tape, corresponding frictional forces are at play. The frictional force F_t at the tape-roller interface is:

$$F_t = \mu T\left(1 - e^{-\mu\theta}\right). \tag{2}$$

The exponential term accounts for the distribution of friction over the contact area. At higher wrapping angles $(\theta \gg 1)$, the frictional force approaches its maximum value, $F_t \approx \mu T$.

The tangential force F_{tan} due to tape motion is:

$$F_{tan} = \rho_t A_t v_t^2, \tag{3}$$

where ρ_t is the tape's material density, and $A_t = b{\cdot}h$ is the cross-sectional area of the tape.

2.2. Sources of Error in Raster Scale Formation

Despite the numerous factors influencing the formation of raster structures within the device, which affect the accuracy of the produced scale, this study focuses on investigating the slippage of the metal tape in the measurement roller surface and the impact of mechanical vibrations.

2.2.1. Slippage

Slippage refers to the relative motion between the tape and the measuring roller, where the tape moves without maintaining a perfect one-to-one correspondence with the roller's rotational motion. This phenomenon occurs when the tangential force F_{tan} at the tape-roller interface exceeds the maximum static friction force F_t, resulting in a loss of synchronization between the tape's linear displacement and the roller's angular displacement. Consequently, this misalignment leads to positional errors during the generation of raster elements.

Slippage directly impacts the positional accuracy and geometric quality of the rasters generated on the tape. When slippage happens, the actual position of the tape is different from the expected position based on the roller's angular displacement. This issue is particularly critical in systems where a laser dynamically forms raster elements. In these systems, an angular encoder often synchronizes the laser's activation timing with the tape's position. Slippage disrupts this synchronization, causing the laser to activate too early or too late, which leads to the irregular spacing of shapes in the generated raster.

The interaction between the tape and the measuring roller is also crucial for maintaining consistent velocity measurement. Slippage compromises this consistency, resulting in errors in encoder signal interpretation. If the tape's actual velocity does not match the calculated velocity due to slippage, the machine may produce uneven or distorted raster elements. Moreover, slippage is rarely uniform and can vary due to changing tape tensions, external vibrations, or non-uniform friction. These variations introduce cumulative errors, which worsen over extended periods, severely impacting the reliability of the generated structure.

Slippage often introduces high-frequency oscillations or harmonics in the tape's displacement data. These distortions manifest as high-frequency positional errors, degrading the clarity and regularity of the raster symbols. The cumulative effects of slippage and its associated errors underscore the importance of minimizing slippage to ensure accurate and reliable raster generation.

Slippage is modelled as the deviation between the tape's linear velocity v_t and the roller's angular velocity ω_r. The slippage ratio S is:

$$S = \frac{|v_t - \omega_r r|}{v_t}, \tag{4}$$

Any nonzero slippage ratio directly translates to a proportional error in position estimation. For example, a slippage ratio of 0.01 (1%) implies that every meter of tape movement introduces a 10 mm positional error.

For no slippage, the frictional force F_t must counteract the tangential force F_{tan}:

$$\begin{gathered} F_t \geq F_{tan}, \\ \mu T\left(1 - e^{-\mu\theta}\right) \geq \rho_t A_t v_t^2. \end{gathered} \tag{5}$$

In this case, the system is considered stable. By rearranging this inequality, other important parameters necessary to maintain a stable system without slippage can be defined, such as the critical wrapping angle θ_c, minimum tape tension T_{min}, or a critical tape velocity v_{crit}.

The critical wrapping angle θ_c describes the minimum angle of contact between the tape and the roller required to generate sufficient frictional force to prevent slippage. It ensures that the available frictional force exceeds the tangential forces acting on the tape due to its motion.

$$\theta_c = -\frac{1}{\mu} ln\left(1 - \frac{\rho_t A_t v_t^2}{\mu T}\right), \tag{6}$$

The critical wrapping angle ensures operational stability. If the actual wrapping angle θ exceeds θ_c, slippage is prevented. Conversely, if $< \theta_c$, the available frictional force is insufficient, leading to slippage and positional errors. By making design changes to the rollers or guiding the tape, the wrapping angle can be increased. This makes the system more stable without needing more tension or slower speeds.

The minimum tape tension T_{min} is the baseline tension needed to prevent instability, slippage, and misalignment in raster scale generation. While the required tension is typically very low in well-designed systems, maintaining tension above this threshold is essential to ensure smooth operation and high precision. In practice, higher tensions are often applied to provide a safety margin and further minimize errors. The minimum tape tension T_{min} required to prevent slippage can be obtained by rearranging Equation (5):

$$T_{min} = \frac{\rho_t A_t v_t^2}{\mu\left(1 - e^{-\mu\theta}\right)}, \tag{7}$$

The critical velocity v_{crit} is the maximum linear velocity of the tape at which the tangential forces due to motion are still balanced by the available frictional force at the tape-roller interface. Beyond this speed, the tangential force exceeds the available frictional force, leading to slippage. The critical velocity is one of the most important factors for making sure that systems that move tapes, like raster scale generation, work reliably. Rearranging inequality for the critical velocity:

$$v_{crit} = \sqrt{\frac{\mu T\left(1 - e^{-\mu\theta}\right)}{\rho_t A_t}}, \tag{8}$$

If $F_t < F_{tan}$, slippage occurs, and the relative velocity between the tape and roller becomes nonzero. The relationship between the tape velocity v_t and the roller angular velocity ω_t during slippage is:

$$\Delta v = v_t - \omega_r r = \frac{F_{tan} - F_t}{\zeta}, \tag{9}$$

where Δv is the velocity mismatch, and ζ is the viscous friction coefficient of the tape-roller interface.

Over the time interval Δt, the positional error due to slippage is:

$$\Delta x = \int_0^{\Delta t} \Delta v \, dt, \tag{10}$$

For continuous operation, the total cumulative error over a length L is:

$$\Delta x_{total} = \int_0^{L/v_t} \Delta v \, dt, \tag{11}$$

Effective mitigation strategies, such as optimizing the tape tension, increasing the wrapping angle, and improving roller design, are essential to minimize its adverse effects. Understanding and controlling slippage dynamics ensures high-quality production.

Increasing the wrapping angle enhances friction by enlarging the tape's contact with the roller, stabilizing motion, and reducing velocity mismatches. Maintaining tape tension above the critical threshold prevents slack and misalignment, with dynamic tensioning systems ensuring consistency in real time. Textured rollers or coatings that increase surface friction further reduce slippage, and keeping the surface clean ensures a consistent grip.

Controlling tape velocity within a safe range ensures that tangential forces do not exceed available friction, preserving synchronization and reducing errors. Real-time feedback mechanisms, using sensors to monitor tape displacement and roller velocity, enable active compensation during operation.

By optimizing these parameters and incorporating real-time feedback, slippage-related errors, including positional mismatches and distortions, can be minimized. This ensures the production of precise, high-quality raster scales for advanced linear measurement systems.

2.2.2. Mechanical Vibrations

In raster scale generation, vibrations are the oscillating movements of the stainless-steel tape that happen both longitudinally (along the tape's length) and transversely (across the tape's plane). There are many things that can cause these vibrations, such as mechanical noise from the environment or nearby machines, problems inside the machine (like a broken drive mechanism, uneven tape tension, or rollers that do not line up properly), and operational factors (like fast tape movements and loading that comes and goes during raster generation). These dynamic effects significantly impact the precision and accuracy of raster scales.

Vibrations can cause positional errors by introducing periodic deviations in the tape's position, which lead to the misplacement of raster elements. These errors manifest as irregular spacing between raster patterns and misaligned symbols, degrading measurement accuracy. In addition, high-frequency vibrations cause harmonic distortions that change the raster geometry in a way that looks like ripples and makes the patterns less clear and uniform. Over longer scales, even small deviations accumulate, leading to substantial misalignment and non-uniform spacing.

Longitudinal vibrations are described by a one-dimensional wave equation:

$$\frac{\partial^2 u(x,t)}{\partial t^2} = c_l^2 \frac{\partial^2 u(x,t)}{\partial x^2}, \tag{12}$$

where $u(x,t)$ represents the longitudinal displacement, $c_l = \sqrt{\frac{E_t}{\rho_t}}$ is the longitudinal wave speed, E_t is the Young's modulus of the tape material, and ρ_t is the tape density.

For a tape of length L, fixed at both ends $(u(0,t) = 0; u(L,t) = 0)$, the natural frequencies of longitudinal vibrations are given by:

$$f_{n,l} = \frac{nc_l}{2L}, \quad n = 1,\ 2,\ 3,\ldots \tag{13}$$

where n represents the vibration mode number. Transverse vibrations follow the equation:

$$\frac{\partial^2 v(x,t)}{\partial t^2} + 2\zeta \frac{\partial v(x,t)}{\partial t} + \omega_n^2 v(x,t) = \frac{T}{\rho_t A_t} \frac{\partial^2 v(x,t)}{\partial x^2}, \tag{14}$$

where $v(x,t)$ is the transverse displacement, $\omega_n = 2\pi f_{n,t}$ is the angular frequency of the n-th mode, and ζ is the damping ratio. The fundamental frequency of the transverse vibrations can be seen in Equation (13).

The maximum positional deviation due to transverse vibrations is:

$$\Delta x_{max} = V_n \sin\left(\frac{n\pi}{L}\right), \tag{15}$$

where V_n is the amplitude of the nth mode. The cumulative effect over a length L is:

$$\Delta x_{total} = \int_0^L V_n \sin\left(\frac{n\pi}{L}\right) dx, \tag{16}$$

These relationships highlight how vibration-induced errors accumulate over long scales. Several strategies can be employed to reduce the effect of vibrations. Optimizing tape tension is a primary method. Increasing tension raises the natural frequency of vibrations, moving it out of the operational range and avoiding resonance. Real-time dynamic tension control systems can maintain optimal tension during operation. Damping techniques also play a crucial role. Vibrations can be absorbed by materials that are naturally damping or by applying damping coatings. Devices that absorb vibrations, such as tuned mass dampers or viscous dampers, can further reduce oscillatory effects.

To lower external excitations, you can isolate the machine's base to cut down on mechanical noise from the outside and make sure the rollers are precise to lower periodic excitations. Adjustments to the way the machine works, like making sure the speed is just right to avoid resonant frequencies and using controlled acceleration or deceleration, stop dynamic loads from causing more vibrations. Structural design enhancements, including rigid machine frames and the use of side guides to stabilize tape motion, further reduce susceptibility to vibrations.

2.3. Summary of System Parameters

To optimize the tape displacement measurement unit and achieve the highest possible process quality, the relevant unit parameters were carefully calculated, evaluated against the whole system's capabilities, and finalized. The optimization process involved assessing factors such as tape tension, roller dynamics, and slippage control minimization. Table 1 presents the key parameters.

Table 1. Assigned and calculated system parameters.

Parameter	Abbreviation	Value	Reference Equation
Measurement roller material	-	Aluminum alloy 6061	-
Measurement roller radius	R	148 mm	-
Metal tape material	-	Stainless-steel AISI 420	-
Density	ρ_t	7800 kg/m^3	-
Young’s Modulus	E_t	200 GPa	-
Tape width	b	8 mm	-
Tape thickness	h	0.2 mm	-
Cross-section area	A	1.6×10^{-6} m^2	-
Coefficient of friction	μ	0.3	
Critical wrapping angle	θ_C	$3.6 \times 10^{-7\circ}$	(6)
Wrapping angle	θ	100°	-
Min. Tape tension	T_{min}	1.022×10^{-7} N	(7)
Tape tension	T	22 N	-
Tape critical velocity	v_{crit}	14.68 mm/s	(8)
Tape velocity	v	1 mm/s	-
Friction force	F_t	2.69 N	(2)
Tangential friction force	F_{tan}	1.248×10^{-8} N	(3)

3. Experimental Research of the Dynamic Tape Behavior

Several experiments were conducted to look into the moving behavior of the stainless-steel tape scale, especially to see how much the tape and roller could slip and how mechanical vibrations would affect it. Researchers looked at this tape displacement measuring unit as part of the whole operating system. They looked at how it changed when the tape was moving at its normal linear speed. Additionally, scenarios were analyzed where the tape was subjected to various external mechanical vibrations along its length.

To evaluate the stability of the relative position between the tape and the measuring roller, which directly affects the accuracy of the entire technological process, a comparison was conducted between the readings of the precision angular encoder measuring the roller’s rotation and the readings of the linear encoder head scanning the scale formed on the moving tape. Furthermore, the accuracy of the scale formed on the tape was measured to assess the high-frequency error component.

For the dynamic behavior research, the calibrated vibration measurement instruments were used, including:

- Mobile equipment Type 3660-D (Brüel & Kjær, Darmstadt, Germany) for recording, storage, processing, and handling of measurement results;
- Notebook DELL with appropriate software;
- Three-axis accelerometers Type 4506 (Brüel & Kjær, Darmstadt, Germany);
- Mini-shaker Type 4810 (Brüel & Kjær, Darmstadt, Germany);
- Eddy-current sensor probes U3B (Lion Precision, Minneapolis, MN, USA).

Beeswax attaches accelerometers and the movable components of non-contact displacement sensors to the stainless-steel tape surface and other objects. This method is advantageous due to beeswax’s ability to provide a secure bond while maintaining minimal impact on system dynamics. By applying and compressing the beeswax into a very thin layer, the resonant frequency of the system is only slightly reduced, ensuring reliable measurements.

3.1. Investigation of Vibration Behavior at Operational Rastering Velocity

In this experiment, longitudinal vibrations of the tape moving at an operational speed of $v_t = 1$ mm/s were measured at points located before and after the analyzed tape displacement measurement unit. The dynamic response of the tape was recorded using two three-axis accelerometers (Brüel & Kjær 4506), which were mounted directly on the stainless-steel tape surface. A schematic representation of the experiment is provided in Figure 3.

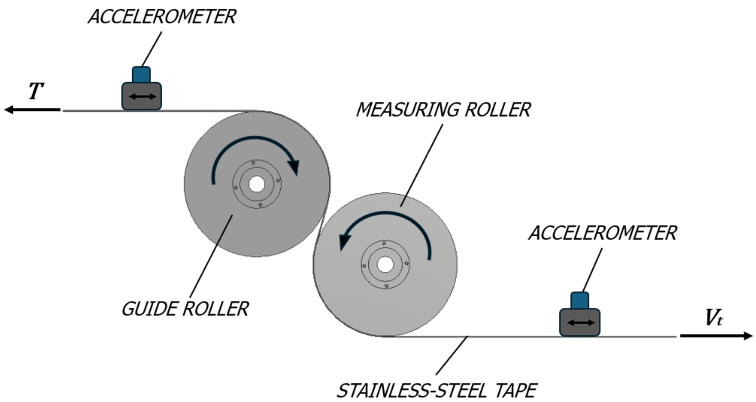

Figure 3. Vibration measurement at the operational velocity, using two accelerometers.

Graphs showing the variation in tape vibrations (in the longitudinal direction) over time and their frequency characteristics are presented in Figure 4.

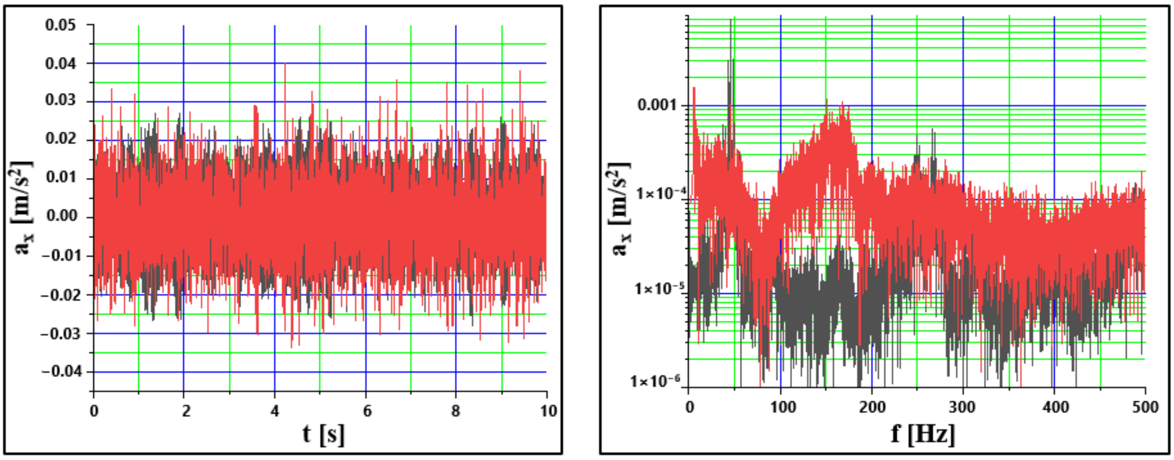

(**a**) (**b**)

Figure 4. Graphs of the tape longitudinal vibrations before (red line) and after (grey line) the tape displacement measurement unit over time (**a**) and their frequency characteristics (**b**).

The results indicate that the tape vibrates with different amplitudes and frequency characteristics before and after the displacement measurement unit. These observed differences suggest that variations in tape velocity and tension occur, which may lead to tape slippage on the measuring roller.

From the perspective of the problem being addressed, it is crucial to analyze the alignment of the vibrations between the tape enveloping the measuring roller and the measuring roller itself under operational speed conditions. One of the three-axis accelerometers is mounted on the surface of the stainless-steel tape at the point where it wraps the measuring roller, while the other accelerometer is attached to the measuring roller near the enveloping tape. A schematic representation of the experimental setup is presented in Figure 5.

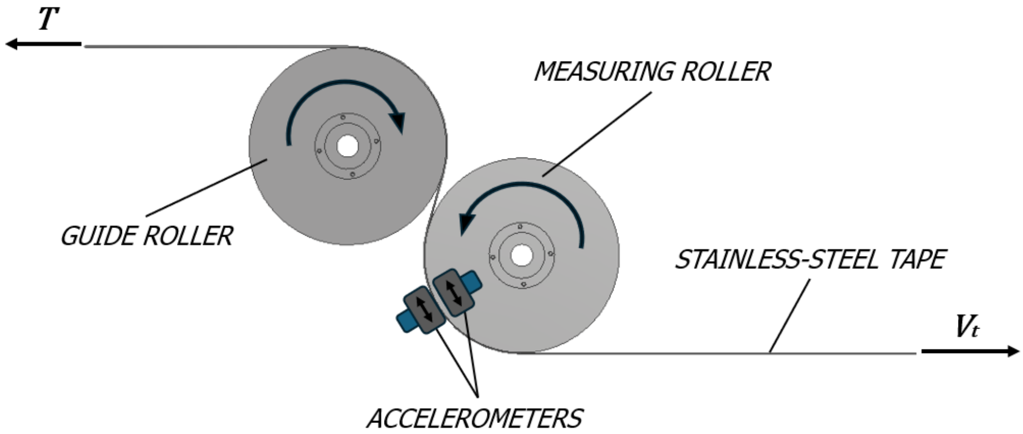

Figure 5. Vibration measurement at the operational velocity using two accelerometers on the measuring roller and the roller enveloping tape.

The measurement results of these vibrations are shown in Figure 6.

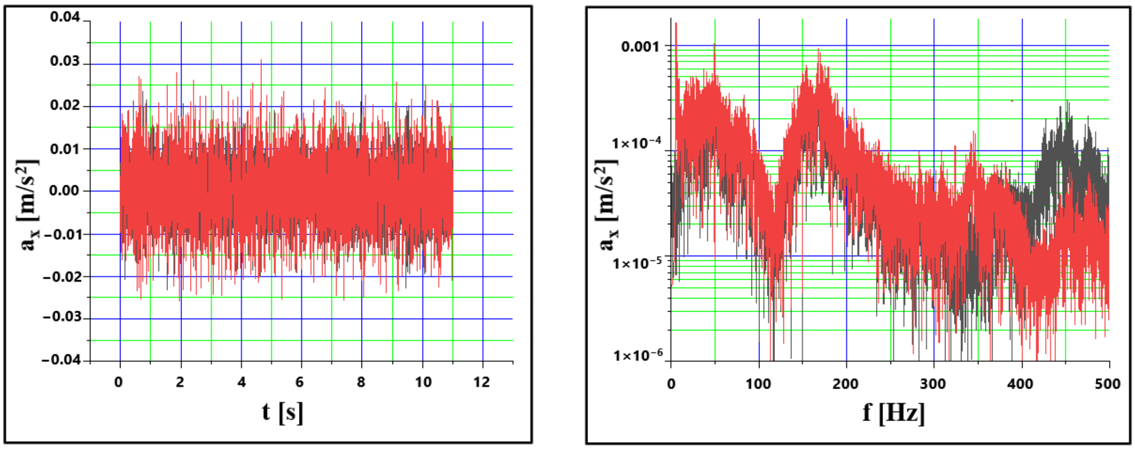

(**a**) (**b**)

Figure 6. Graphs of the tape longitudinal vibrations (red line) and the measuring roller (grey line) unit over time (**a**) and their frequency characteristics (**b**).

An evaluation of the frequency characteristics of the measuring tape and the measuring roller reveals a strong correlation at low and medium frequencies. This shows that the dynamics are stable within these ranges, which means that there probably is not going to be any major systematic slippage that could cause errors. The close alignment of these characteristics demonstrates effective interaction between the tape and the roller under normal operating conditions.

3.2. Investigation of Vibration Behavior at Forced Longitudinal Vibrations

To study the dynamics of forced longitudinal vibrations in the tape displacement measurement unit, a controlled setup is employed where a mini-shaker's (Brüel & Kjær Type 4810) rod is attached to the free end of the tape. This configuration ensures that vibrations are induced directly through the tape. The supporting frame securely mounts the shaker, ensuring stability and precise transmission of oscillatory forces. Figure 7 shows a simplified version of this arrangement. It lets you control how much the tape vibrates, which is similar to what might happen during raster scale generation.

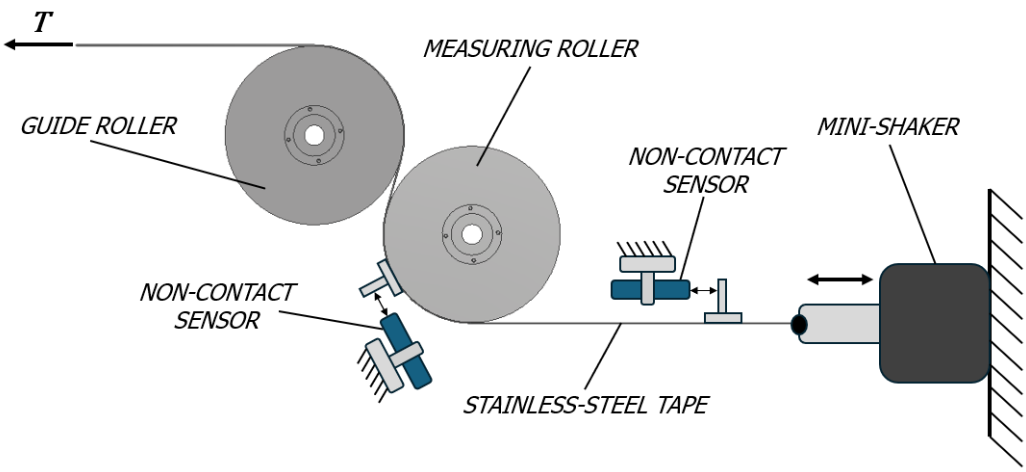

Figure 7. Vibration measurement at forced longitudinal vibrations in the tape displacement measurement unit.

Tape vibrations are measured using two high-precision non-contact displacement sensors (Lion Precision U3B), specifically designed for detecting small displacements. Its compact size and low mass preserve the natural vibration characteristics. One sensor's movable element is attached to the surface of the tape enveloping the measurement roller, while the other is positioned on the tape near the mini-shaker. This setup ensures precise monitoring of the system's dynamic behavior.

For more research, the tape was excited with vibrations of varying frequencies (called "sweep") between 20 Hz and 600 Hz, as well as vibrations at the known resonant frequencies. Figure 8 presents the results of the tests conducted in the "sweep" mode.

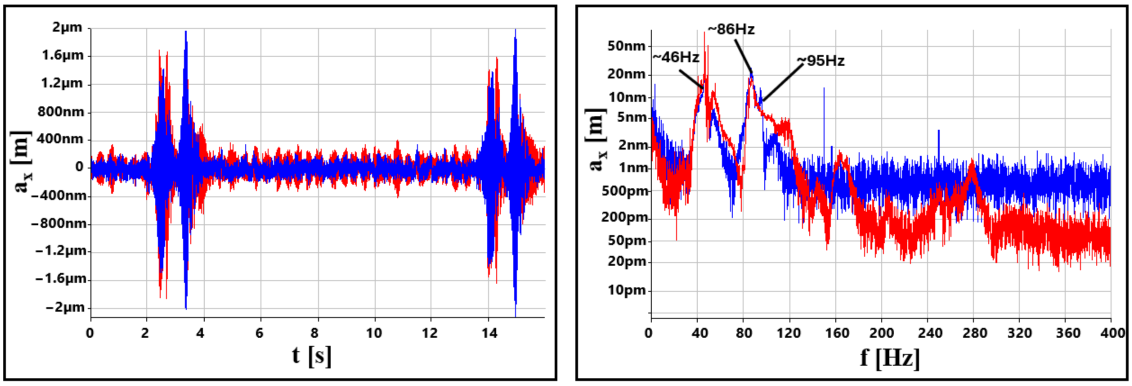

(**a**) (**b**)

Figure 8. Graphs of tape longitudinal vibrations under the forced "sweep" mode excitation over time (**a**) and its amplitude-frequency characteristics (**b**), measured at the locations where tape wraps the measurement roller (blue line) and next to the mini-shaker (red line).

From the "sweep" test, the resonant frequencies of the system were identified. Peaks in vibration amplitude were observed at 46.19 Hz with an amplitude of 27.20 nm, at 86.44 Hz with an amplitude of 43.13 nm, and at 94.75 Hz with an amplitude of 15.72 nm. Other vibration maxima up to 400 Hz did not exceed 13 nm.

3.3. Relationship Between Tape Linear Velocity and Tangential Velocity of the Measuring Roller's Peripheral Point

The variation in the tape's linear velocity along its length and its correlation with the peripheral velocity of a point on the measuring roller is analyzed. In this case, an optical linear encoder reading head (FAGOR ITRY) measures the tape's displacement within the raster formation zone. The reading head is mounted and precisely aligned above the tape surface, which has a pre-formed 20 μm incremental raster scale. The resolution of the read head's output signals (TTL) reaches 0.5 μm.

Simultaneously, output signals from a specially designed high-precision angular encoder mounted on the measuring roller are recorded. After interpolation of the encoder's analog output signals (1Vpp), the angular encoder achieves a resolution of 3,600,000 counts per revolution. Figure 9 displays the schematic diagram of the experimental setup.

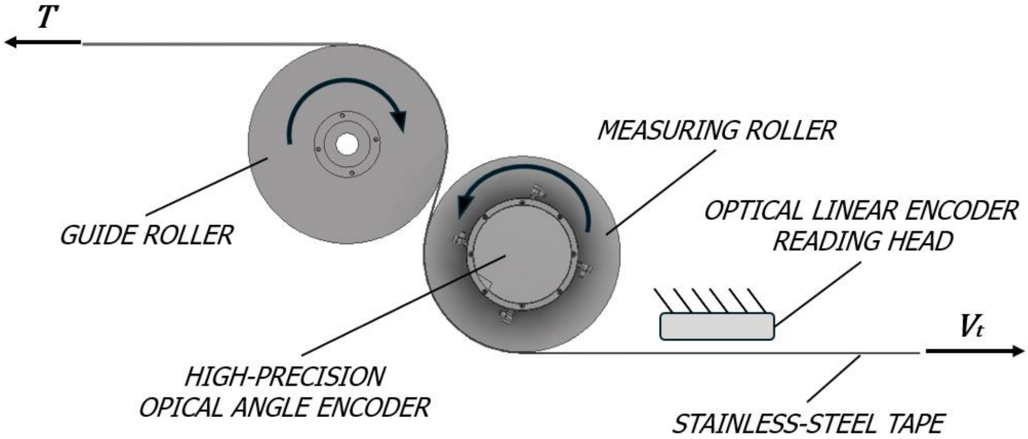

Figure 9. The principal scheme of the experiment is to determine the relationship between tape linear velocity and the rotation velocity of the measuring roller.

During the experiment, the tape was pulled at the operational raster formation speed v_t. The tape's displacement velocity in the raster formation zone was measured according to the number of linear encoder pulses per unit of time. Similarly, we expressed the tangential velocity of the measuring roller's peripheral point as the number of high-precision angular encoder pulses during the same time period. The pulse counting period was set to 10 ms.

Over 9000 readings, a total of 174,717 linear encoder pulses were recorded, with an average of 19.413 pulses per 10 ms period. Considering the encoder's resolution of 0.5 μm, the calculated tape displacement speed was 0.97065 mm/s. The root mean square (RMS) deviation of the velocity from the mean value was ±0.1080 mm/s. Assuming a confidence interval of 2.1 RMS deviations (corresponding to a 96% probability), the tape's displacement velocity was determined to be 0.97065 ± 0.2268 mm/s. This indicates that the velocity varied from 0.74385 mm/s to 1.19745 mm/s, corresponding to a variation of ±22.01% relative to the mean value. Figure 10 presents the variation in the measured number of pulses every 10 ms.

For the same tape displacement, a total of 338,047 angular encoder pulses were recorded, with an average of 37.56067 pulses per 10 ms period. By looking at the number of pulses from both encoders and the fixed resolution of the linear encoder (0.5 μm), the resolution of the angular encoder was made better. One pulse from the angular encoder corresponds to a displacement of 0.25842 μm at the peripheral point of the measuring roller. The root mean square (RMS) deviation of the velocity variation relative to the mean value was calculated to be ±0.0934 mm/s. Assuming a confidence interval of ±2.1 RMS deviations (96% probability), the tape's displacement velocity was determined to be 0.97065 ± 0.1962 mm/s. This means the velocity ranged from 0.7994 mm/s to 1.16715 mm/s, corresponding to a variation of ±19.26% relative to the mean value. Figure 11 presents the variation in the measured number of pulses every 10 ms.

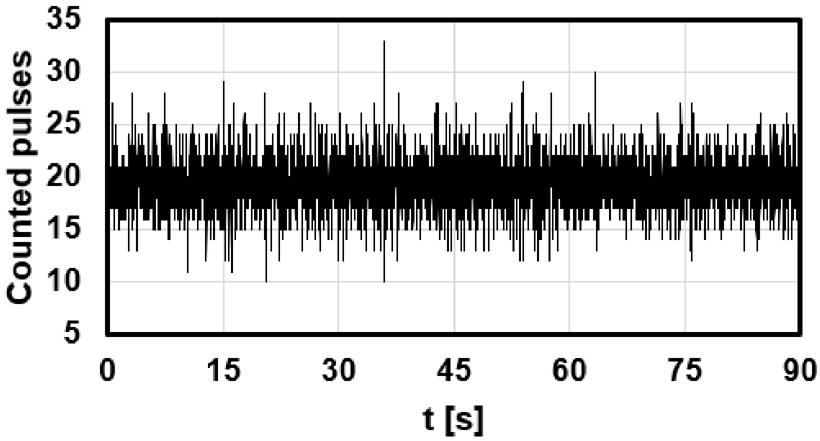

Figure 10. Change in the number of pulses from the linear encoder reading head in 10 ms time intervals.

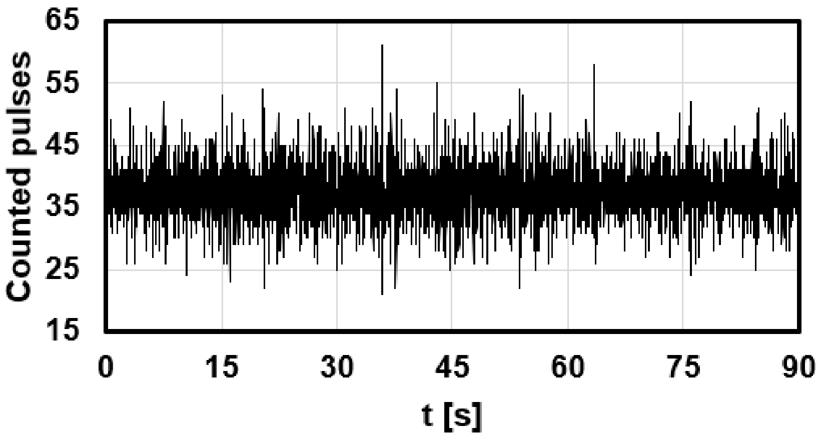

Figure 11. Change in the number of pulses from the optical angular encoder in 10 ms time intervals.

The graphs clearly show the same changes in speed and show that there is a connection between the number of pulses recorded by the angular encoder and those recorded by the linear encoder. To objectively evaluate this relationship, the correlation coefficient was calculated, yielding a value of 0.7948523. This number is very close to 1, and there is not much difference between the speed of the tape pulling and the speed of the measuring roller's edges. This means that the measuring roller's motion is very close to the speed of the tape's displacement, with only a small difference. This small variation is likely attributed to tape deformations caused by fluctuations in the tensile force applied to the tape.

The displacement difference Δd between the raster generating point and the measuring roller was calculated using the following formula:

$$\Delta d = k \cdot n_l - n_k, \tag{17}$$

where k is the ratio of the total number of pulses from the angular encoder to the linear encoder ($\frac{n_k}{n_l} = 1.934826$), n_k is the total number of counted pulses from the high-precision angular encoder, and n_l is the total number of pulses counted from the linear encoder.

The results of this calculation are graphically presented in Figure 12.

It was found that one pulse from the angular encoder causes the tape to move by 0.25845 μm. This meant that the difference in movement between the raster generating point and the measuring roller had to be turned back into linear values. This difference varies within ±2.07 μm. Analyzing the data reveals no clear evidence of systematic slippage.

However, the velocity fluctuations indicate a periodic variation in the difference between the tape's velocity and the measuring roller's velocity.

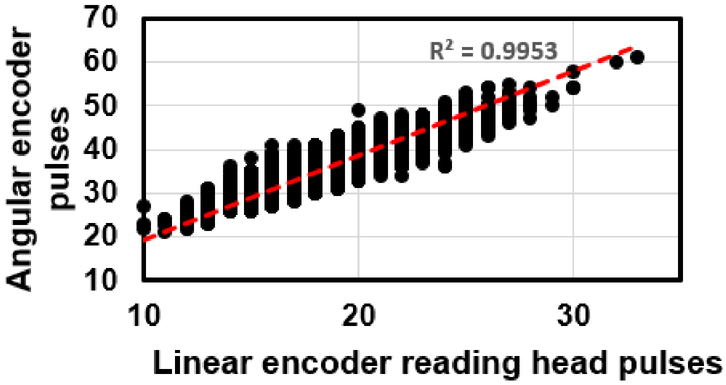

Figure 12. The relationship between the number of pulses read by the angular encoder and the number of pulses from the linear encoder reading head. The red line presents the best-fit linear trendline with a displayed R^2 value.

3.4. High-Frequency Error Component

In order to obtain a better idea of the position errors of individual lines and to reduce the effect of raster line detection errors on the measurements, each step was looked at over a 2 mm length. The tape's accuracy was evaluated using a high-precision comparator, which optically detects the midline of the steps in the formed raster structures and compares their position to a reference provided by the XL-80 laser interferometer (Renishaw, Wotton-under-Edge, United Kingdom) system. The stainless-steel tape's surface forms an incremental raster structure with an integrated zero mark that repeats every 50 mm.

Six realizations were performed for this purpose. Figure 13 graphically presents the results of these measurements.

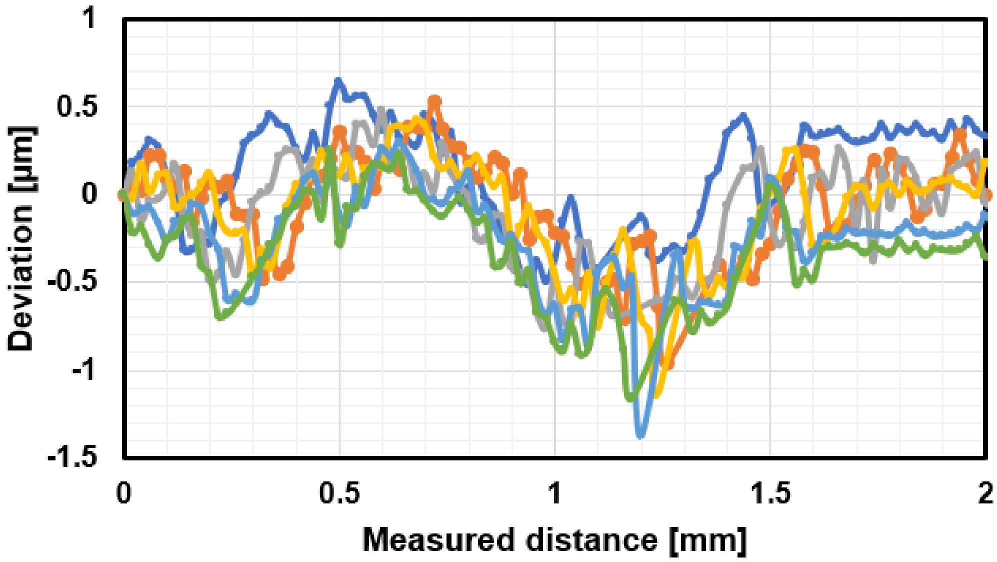

Figure 13. The positional error of raster structure lines over a 2 mm length across six realizations.

Additionally, an average graph was calculated (Figure 14), which provides the clearest representation of the position errors of individual raster lines.

The results of this study indicate that the position error of the lines over a 2 mm length does not exceed 1 µm or ±0.5 µm. The maximum distance between adjacent lines is up to 0.12 µm, with the most probable error range being between 0.05 µm and 0.1 µm.

Larger error Δ_{MAX}, reaching up to 0.2 µm, are observed in the zero-pulse region between 1.1 mm and 1.4 mm. The root mean square (RMS) deviation of the measurement results across different realizations compared to their mean value can be used to figure out how inaccurate the lines' detection is. This RMS is calculated as 0.201 µm. The uncertainty of line detection, with a coverage factor of 2.1 (corresponding to a 96% confidence level), is equal to ±0.44 µm.

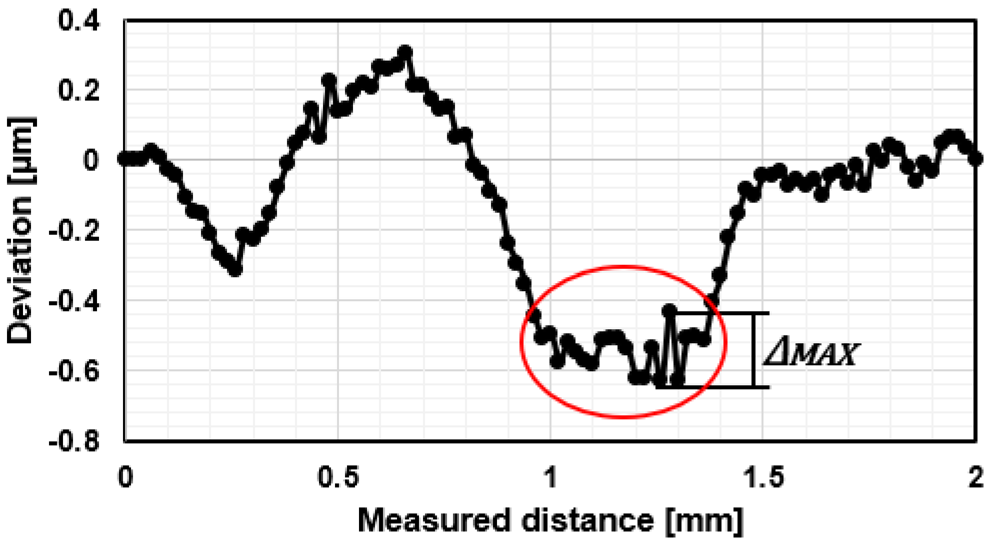

Figure 14. The average positional error of raster structure lines over a 2 mm length across six realizations.

4. Conclusions

A raster-forming technological device with a redesigned tape displacement measurement unit, in which the tape wraps around and drives the measuring roller, has been investigated. Key sources of error in this configuration, such as slippage and mechanical vibrations, were analyzed. Critical parameters of the unit were analytically identified to optimize its performance and minimize the possibility of tape slippage. Experimental tests were conducted to evaluate the mechanical vibrations of the tape under operational conditions and external mechanical excitation. Additionally, the real tape velocity in the raster forming zone was analyzed and compared with the velocity recorded by the measuring roller.

The results support the following conclusions:

1. The dynamic behavior of the tape indicates that variations in tape velocity and its stretching occur during the raster formation process.
2. Despite the observed variations in tape velocity, the strong correlation between the measured tape velocity in the operational raster forming zone and the velocity determined by the tape displacement measurement unit shows that significant systematic tape slippage was not detected. This confirms the reliability of the redesigned unit in maintaining consistent tape movement.
3. Under comparable operational conditions, the results achieved with the redesigned tape displacement measurement unit are significantly better than those of the previous design. The unit exhibited an absolute peak-to-peak error of ±1 µm over a 2 mm length, with a maximum positional error of 0.8 µm between adjacent rasters. In contrast, the redesigned unit achieved improved accuracy, with errors reduced to ±0.5 µm and 0.2 µm, respectively.

Further studies should focus on the stability of tape tension, as current findings suggest that tension variations might contribute to the observed errors. Additionally, looking into the optical angular encoder's internal subdivision error (SDE) would be helpful in seeing how it affects the accuracy of the determined tape speed and positioning. These studies might provide deeper insights into error sources and further enhance the precision and reliability of the system.

Author Contributions: Conceptualization, D.G., A.K. (Albinas Kasparaitis), E.S., J.M. and A.K. (Artūras Kilikevičius); methodology, D.G., A.K. (Albinas Kasparaitis) and A.K. (Artūras Kilikevičius); software, D.G. and A.K. (Artūras Kilikevičius); validation D.G., A.K. (Albinas Kasparaitis), E.S., J.M. and A.K. (Artūras Kilikevičius); formal analysis, D.G., A.K. (Albinas Kasparaitis), E.S., J.M. and A.K. (Artūras Kilikevičius); investigation, D.G., A.K. (Albinas Kasparaitis), E.S., J.M. and A.K. (Artūras Kilikevičius); resources, D.G., A.K. (Albinas Kasparaitis), E.S., J.M. and A.K. (Artūras Kilikevičius); data curation, D.G., A.K. (Albinas Kasparaitis), E.S., J.M. and A.K. (Artūras Kilikevičius); writing—original draft preparation, D.G., A.K. (Albinas Kasparaitis), E.S., J.M. and A.K. (Artūras Kilikevičius); writing—review and editing, D.G., A.K. (Albinas Kasparaitis), E.S., J.M. and A.K. (Artūras Kilikevičius); visualization, D.G., J.M. and A.K. (Artūras Kilikevičius); supervision, A.K. (Albinas Kasparaitis) and A.K. (Artūras Kilikevičius); project administration, D.G., A.K. (Albinas Kasparaitis), E.S., J.M. and A.K. (Artūras Kilikevičius); funding acquisition, E.S. All authors have read and agreed to the published version of the manuscript.

Funding: This research was supported by the Joint Research Collaborative Seed Grant Program between the National Taipei University of Technology and Vilnius Gediminas Technical University (Grant No: TAIPEI TECH-VGTU-2023-02).

Data Availability Statement: The original contributions presented in the research are included in the article. Further inquiries can be directed at the authors.

Conflicts of Interest: The authors declare no conflicts of interest.

References

1. Li, X.; Zhao, J.; Wang, Y. Measurement-Assisted Assembly Techniques for Large Aerospace Structures. *J. Aerosp. Eng.* **2021**, *34*, 456–467.
2. Chen, L.; Zhang, H.; Wei, X. High-Accuracy Optical Encoders for Long-Span Displacement Measurement. *Int. J. Autom. Control* **2020**, *12*, 233–245.
3. Zhang, T.; Liu, K.; Ma, Q. Coordinate Measuring Machine Applications in Large-Scale Machining Systems. *Precis. Eng.* **2019**, *47*, 310–318.
4. Lee, H.; Park, J.; Kim, S. Inkjet Printing Techniques for Scalable Fabrication of Linear Measurement Patterns. *J. Ind. Print.* **2018**, *14*, 98–105.
5. Smith, A.; Brown, T.; Johnson, L. Mechanical Methods for Creating Durable Linear Measurement Scales. *Ind. Eng. J.* **2017**, *33*, 256–272.
6. Ramesh, S.; Patel, K.; Zhao, W. Embossing Technologies for Precision Pattern Creation. *J. Mater. Process. Technol.* **2016**, *221*, 75–89.
7. Chen, Y.; Zhou, H. Ultraviolet Lithography and Its Applications in Microstructure Fabrication. *Microfabr. Technol.* **2020**, *12*, 102–116.
8. Kobayashi, T.; Saito, M.; Nakamura, H. Advances in Laser Ablation for Precision Manufacturing. *J. Precis. Eng.* **2019**, *45*, 213–225.
9. Li, X.; Wang, J.; Tang, Z. Comparative Study of Lithography and Laser Ablation for Precision Scale Production. *Manuf. Process. Rev.* **2021**, *18*, 87–96.
10. Fursenko, A.; Kilikevičienė, K.; Kilikevičius, A.; Skeivalas, J.; Kasparaitis, A.; Matijošius, J.; Wieckowski, D. Analysis of Dynamic Parameters of the System of Raster Formation and Control. *Commun. Sci. Lett. Univ. Žilina* **2020**, *22*, 78–88. [CrossRef]
11. Fursenko, A.; Kilikevičius, A.; Kilikevičienė, K.; Borodinas, S.; Kasparaitis, A.; Matijošius, J. Investigation of Roller-Tape Contact Pair Used in Precision Mechatronic System. *Appl. Sci.* **2020**, *10*, 4041. [CrossRef]
12. Fursenko, A.; Kilikevičius, A.; Kilikevičienė, K.; Kasparaitis, A. Experimental Investigation of Friction Transition on Vibration of Steel Tapes. *AIP Conf. Proc.* **2018**, *2027*, 020001.
13. Brake, M.R.; Wickert, J.A. Frictional Vibration Transmission from a Laterally Moving Surface to a Traveling Beam. *J. Sound Vib.* **2008**, *310*, 663–675. [CrossRef]
14. Ghayesh, M.H. Stability Characteristics of an Axially Accelerating String Supported by an Elastic Foundation. *Mech. Mach. Theory* **2009**, *44*, 1964–1979. [CrossRef]

15. Shin, K.-H.; Kwon, S.-O. The Effect of Tension on the Lateral Dynamics and Control of a Moving Web. *IEEE Trans. Ind. Appl.* **2007**, *43*, 403–411. [CrossRef]
16. Yang, H.; Engelen, J.B.C.; Pantazi, A.; Häberle, W.; Lantz, M.A.; Müftü, S. Mechanics of Lateral Positioning of a Translating Tape Due to Tilted Rollers: Theory and Experiments. *Int. J. Solids Struct.* **2015**, *66*, 88–97. [CrossRef]
17. Samourgkanidis, G.; Kouzoudis, D. Characterization of Magnetoelastic Ribbons as Vibration Sensors Based on the Measured Natural Frequencies of a Cantilever Beam. *Sens. Actuators A Phys.* **2020**, *301*, 111711. [CrossRef]
18. Ma, L.; Cheng, L. Numerical and Experimental Benchmark Solutions on Vibration and Sound Radiation of an Acoustic Black Hole Plate. *Appl. Acoust.* **2020**, *163*, 107223. [CrossRef]
19. Nandakumar, H.; Mallick, S.P.; Srivastava, S. Sensing High Frequency Sub-Nanometer Vibrations Using Optical Coherence Tomography with Real-Time Profilometry of Multiple Inner Layers. *Opt. Lasers Eng.* **2020**, *127*, 105992. [CrossRef]
20. Blanchet, T.A.; Grzyboski, S.M. Conduction Modeling of Multi-Track Raster Scanning of Heat Over a Rectangular Surface Region. *J. Manuf. Process.* **2020**, *52*, 165–180. [CrossRef]